Algorithms to Improve the Standard Atmospheric Correction of SGLI Ocean-Color Imagery and to Compute the Fraction of PAR absorbed by Phytoplankton

Robert Frouin[1], Cécile Dupouy[2], Bruno Pelletier[3]

[1]Scripps Institution of Oceanography, USA

[2]Institute for Research and Development, New Caledonia

[3]University of Rennes, France

Joint GCOM-C PI Workshop, 14 - 17 January 2014, Tokyo, Japan

Issues with the Standard Atmospheric Correction Algorithm

-Adjacency effects

-Turbid waters

-Absorbing aerosols

-Sun glint

-Clouds

-The ocean-color inverse problem is ill-posed, i.e., a large set of ocean and atmospheric states, or pre-images, may correspond to very close values of the satellite signal.

$$\rho \approx \rho_a + \rho_w T_a$$

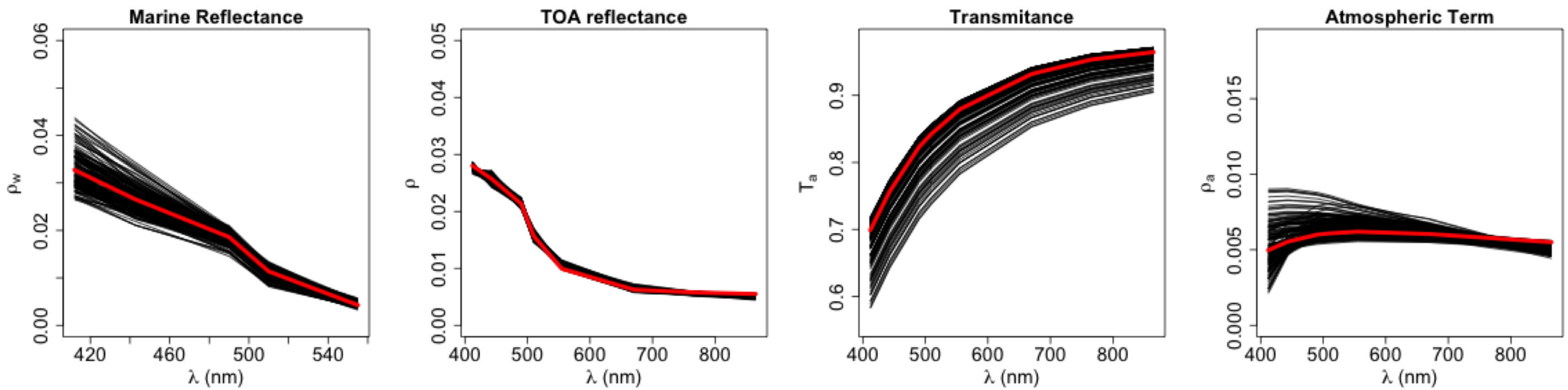

Example of pre-images. Actual values of ρ_w , ρ, T_a, and ρ_a are displayed in red, and the pre-images at a distance no more than δ= 0.001 are displayed in black. The search spaces for the pre-images include NOMAD and AERONET-OC data sets and maritime, continental, and urban aerosols in various proportions and amount.

Bayesian Methodology for Ocean-Color Remote Sensing

<u>Approach</u>

-Noisy TOA reflectance measurement:
$\rho = \phi(\rho_w, x_a) + \varepsilon$

-Prior probability distributions for ρ_w and x_a and noise probability distribution:
$\rho_w \sim P_{0w}$; $x_a \sim P_{0a}$; $\varepsilon \sim P_\varepsilon$

-Bayesian solution (posterior probability distribution): $P(\rho_w/\rho)$, from which expected value and covariance (a measure of uncertainty) can be computed.

-Situations for which forward model and observation are incompatible are also identified (p-value).

Tasks:

-Specify prior distributions P_w and P_a

Assumed uniform for all parameters except aerosol optical thickness (log-normal); ρ_w from NOMAD and AERONET-OC; aerosol parameters from models

-Estimate P_ε

By comparing TOA values from selected imagery with forward model predictions

-Approximate numerically expectation and covariance

Using partition-based models

Theoretical Performance

Average Errors

Geometry-averaged statistics: ρ_w bias and standard deviation per channel, averaged over all the geophysical conditions and observation geometries.

Wavelength (nm)	412	443	490	510	555	670
Average Bias	1.81E-09	-8.06E-10	3.48E-09	3.06E-10	-1.08E-08	-4.66E-09
Average Standard Deviation	0.004321	0.003564	0.003220	0.002936	0.002652	0.001145

Errors per viewing geometry

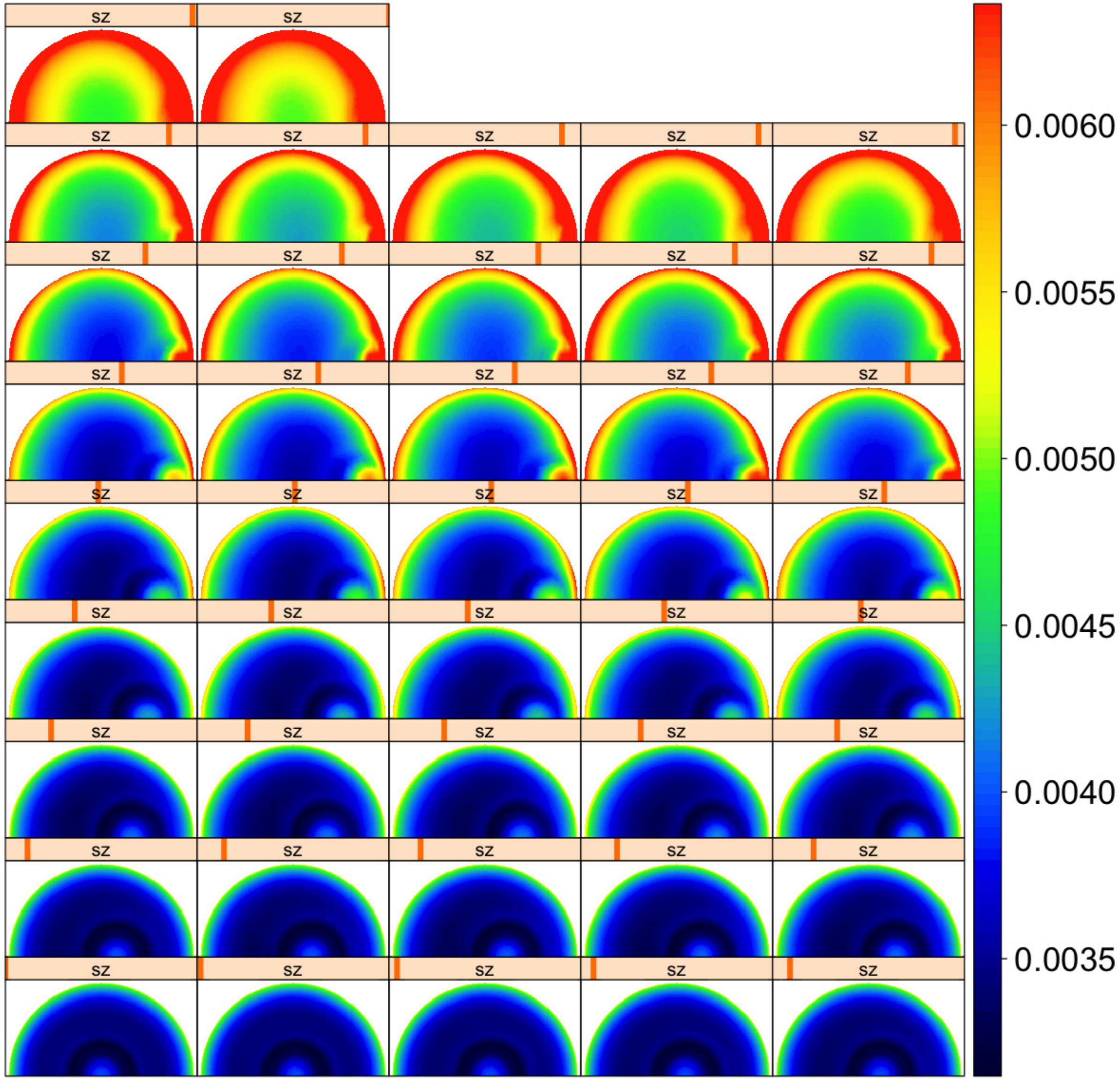

Standard deviation for each angular geometry at 412 nm.

Errors per aerosol optical thickness

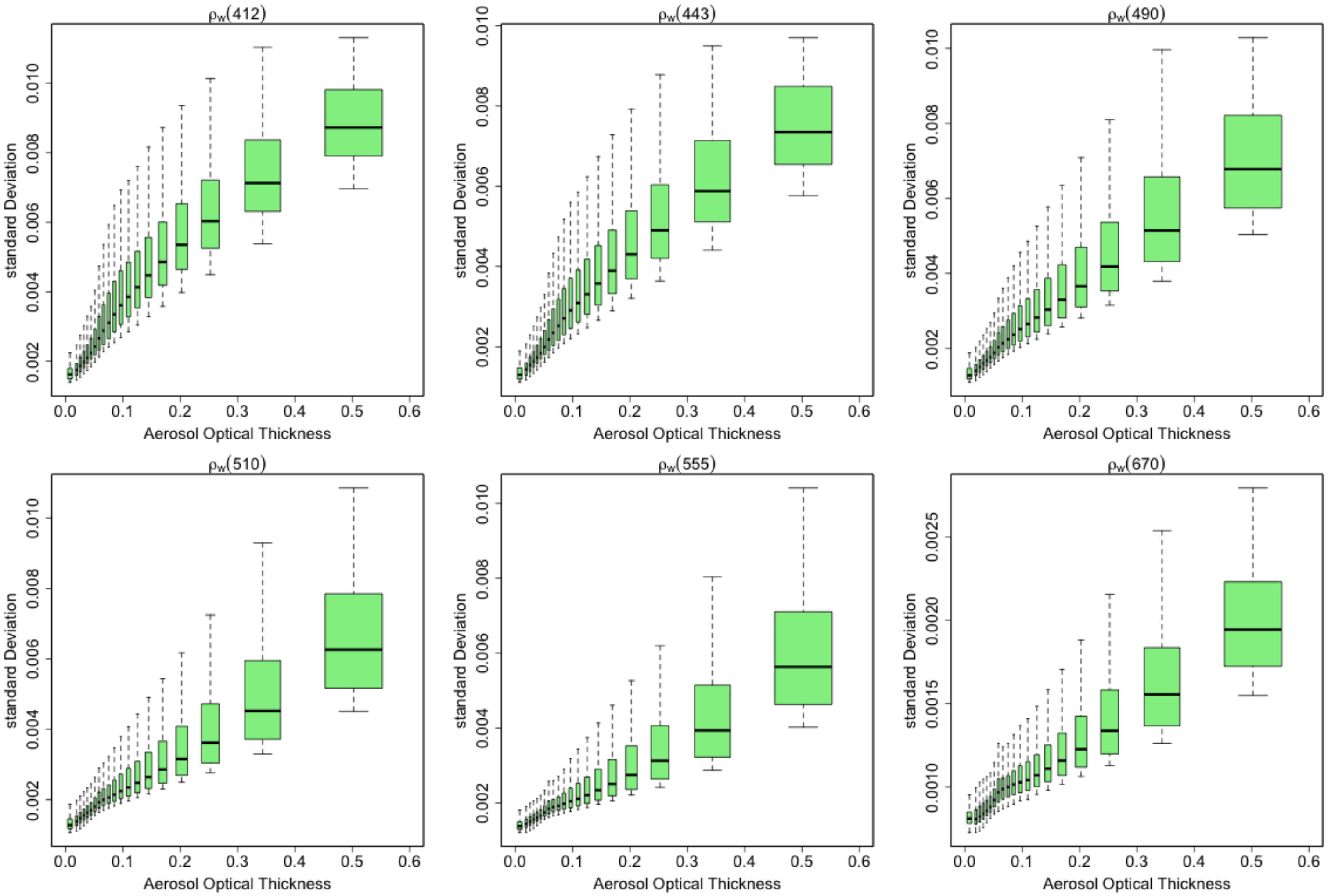

Standard deviation per spectral band aerosol optical thickness bin, with all the geometries.

Errors per aerosol type

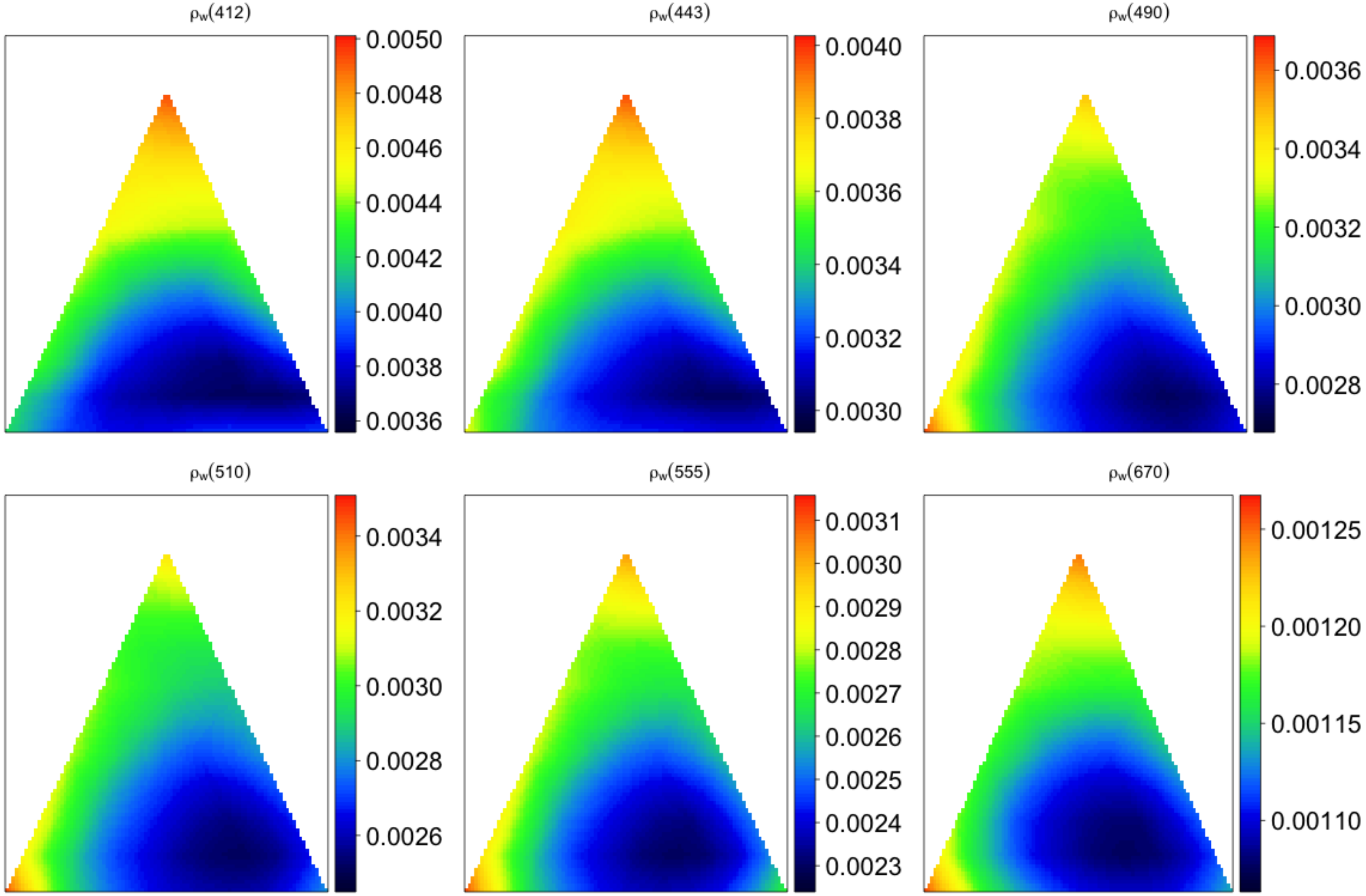

Standard deviation per spectral band, averaged all geometries, as a function of the aerosol type. Maritime aerosols: right corner of triangles, urban: top corner, and continental: left corner.

Application to SeaWiFS imagery

South Africa,
02/14/1999

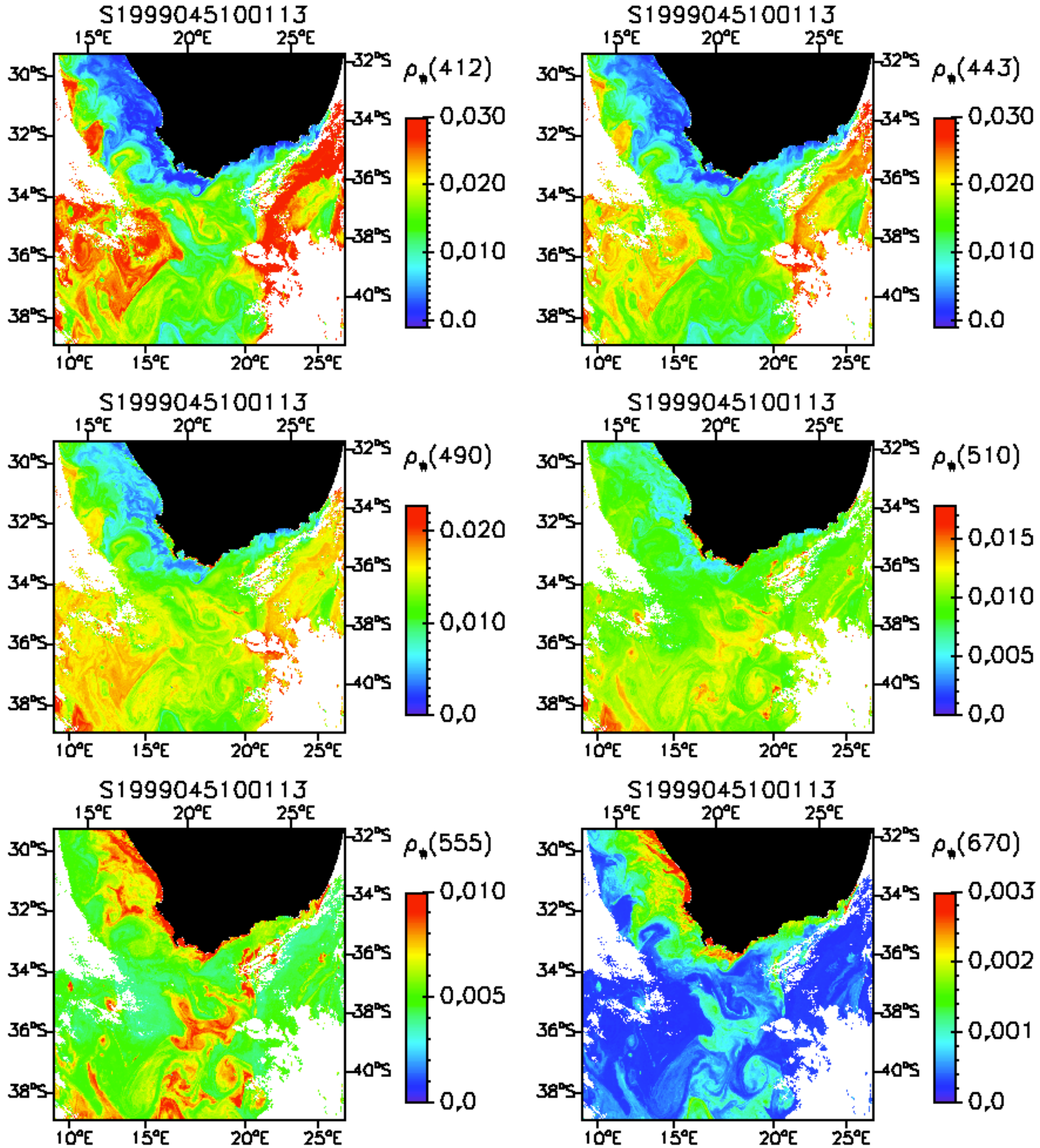

Estimated marine reflectance, Bayesian methodology.

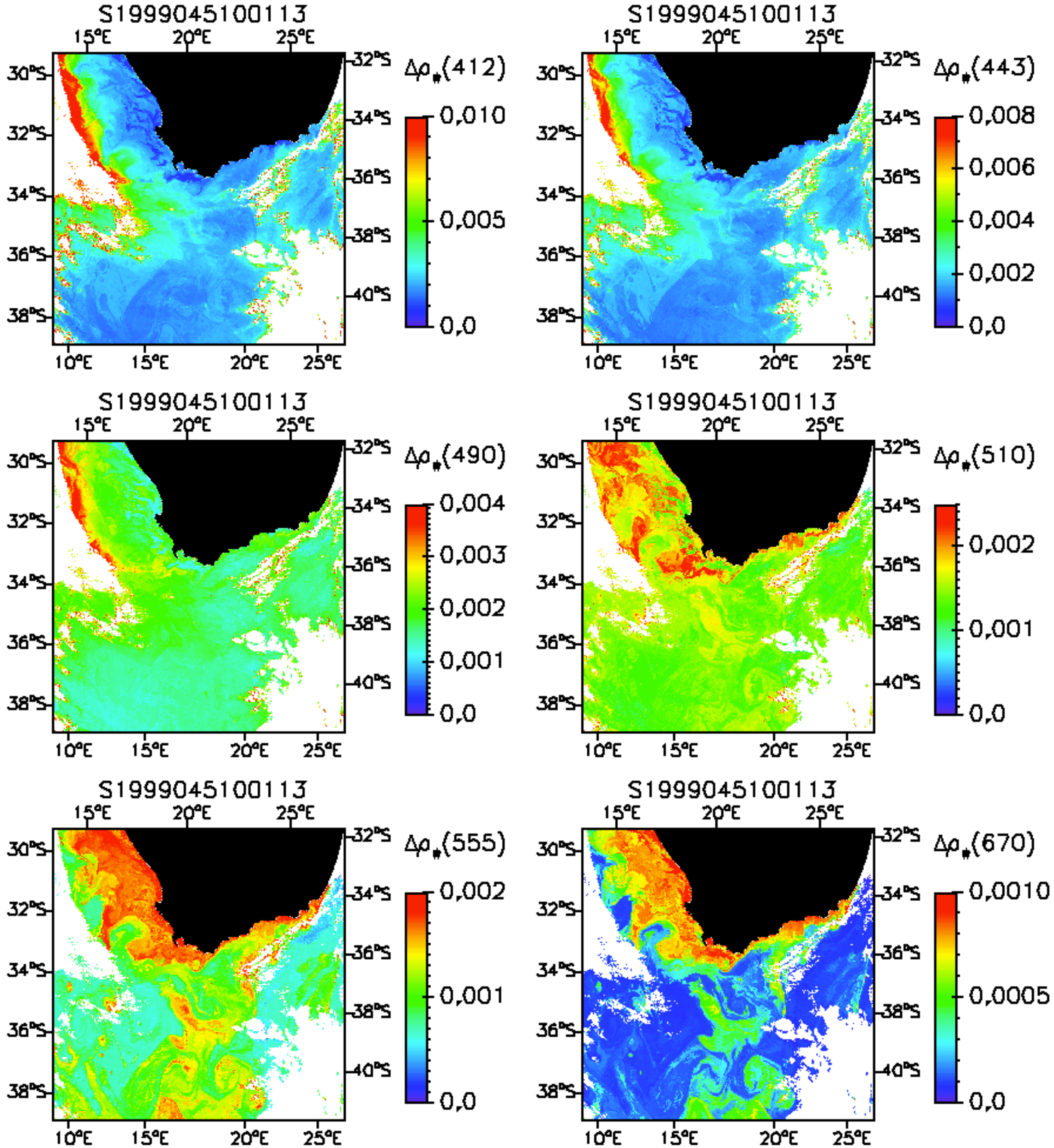

Estimated uncertainty on marine reflectance, Bayesian methodology.

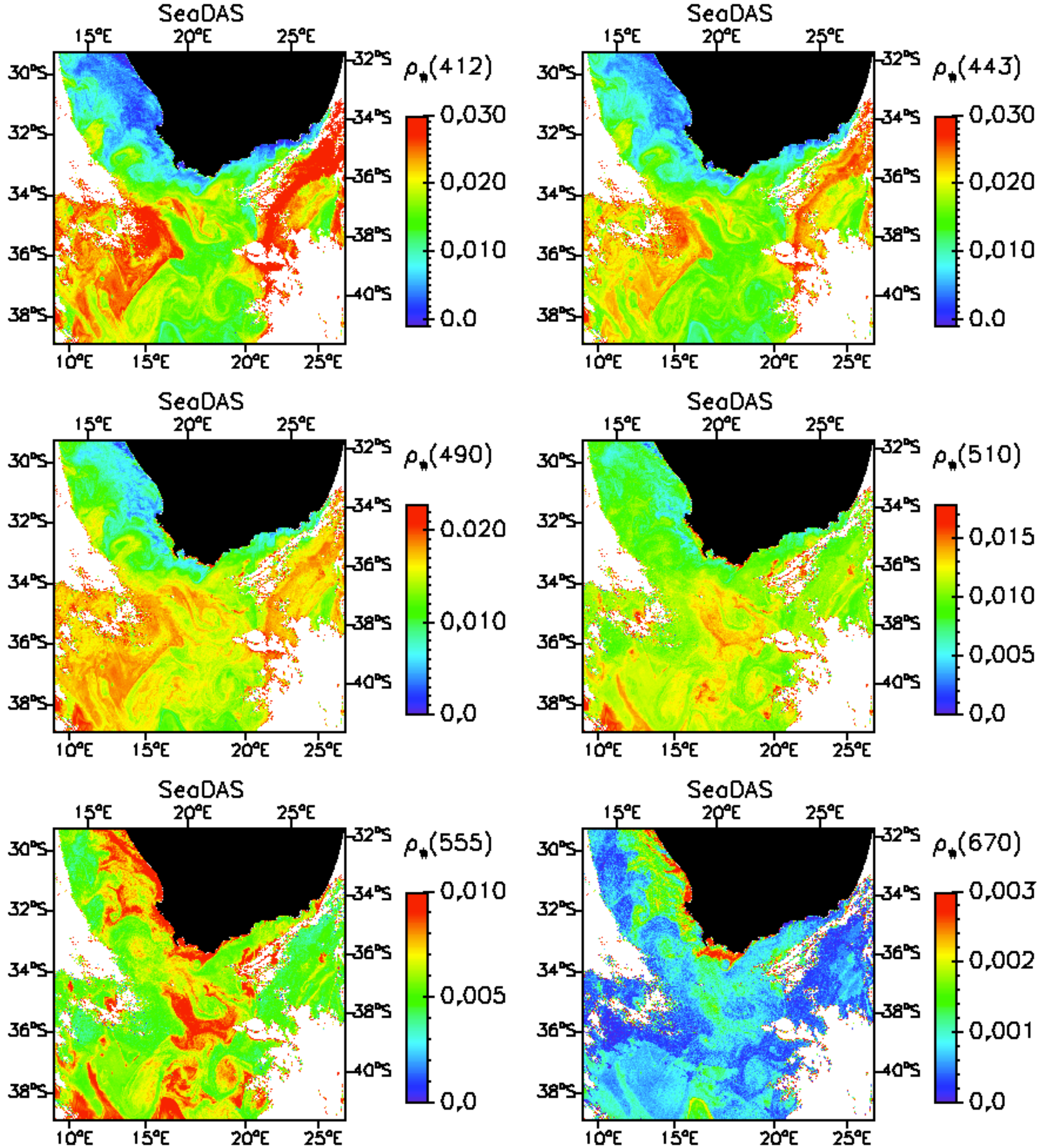

Estimated marine reflectance, SeaDAS algorithm.

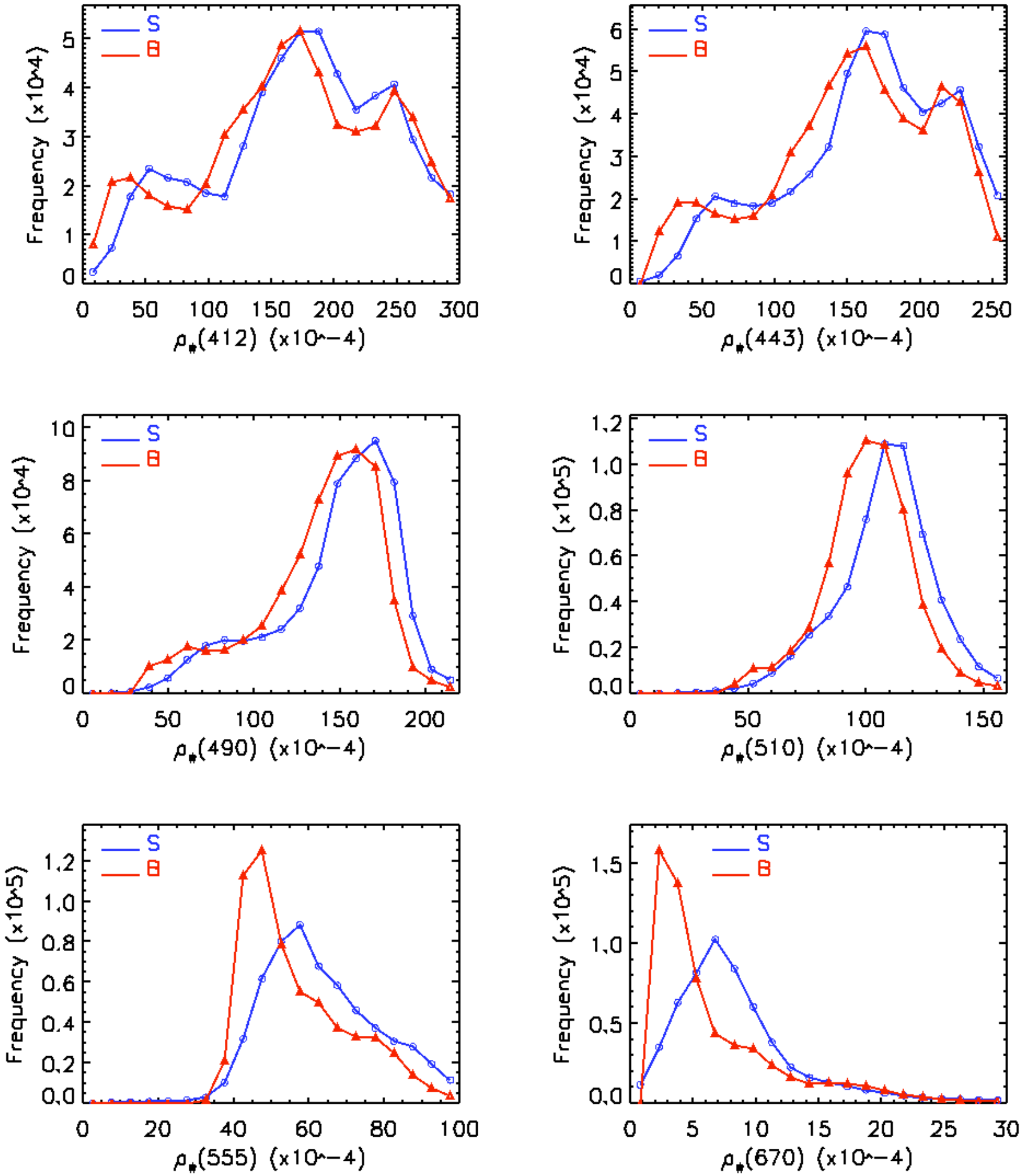

Histograms of valid marine reflectance estimates.

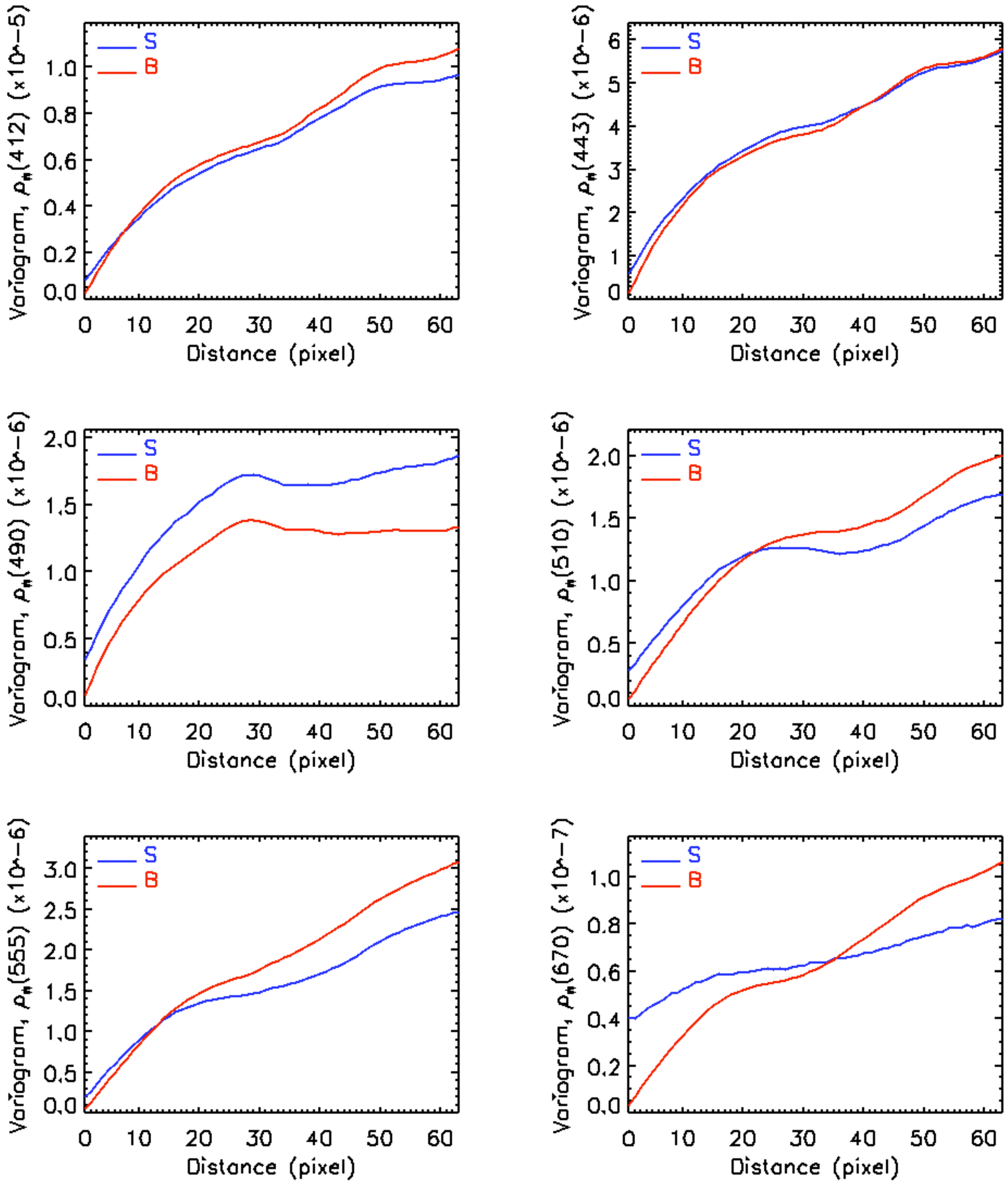

Variograms of valid marine reflectance estimates in selected area.

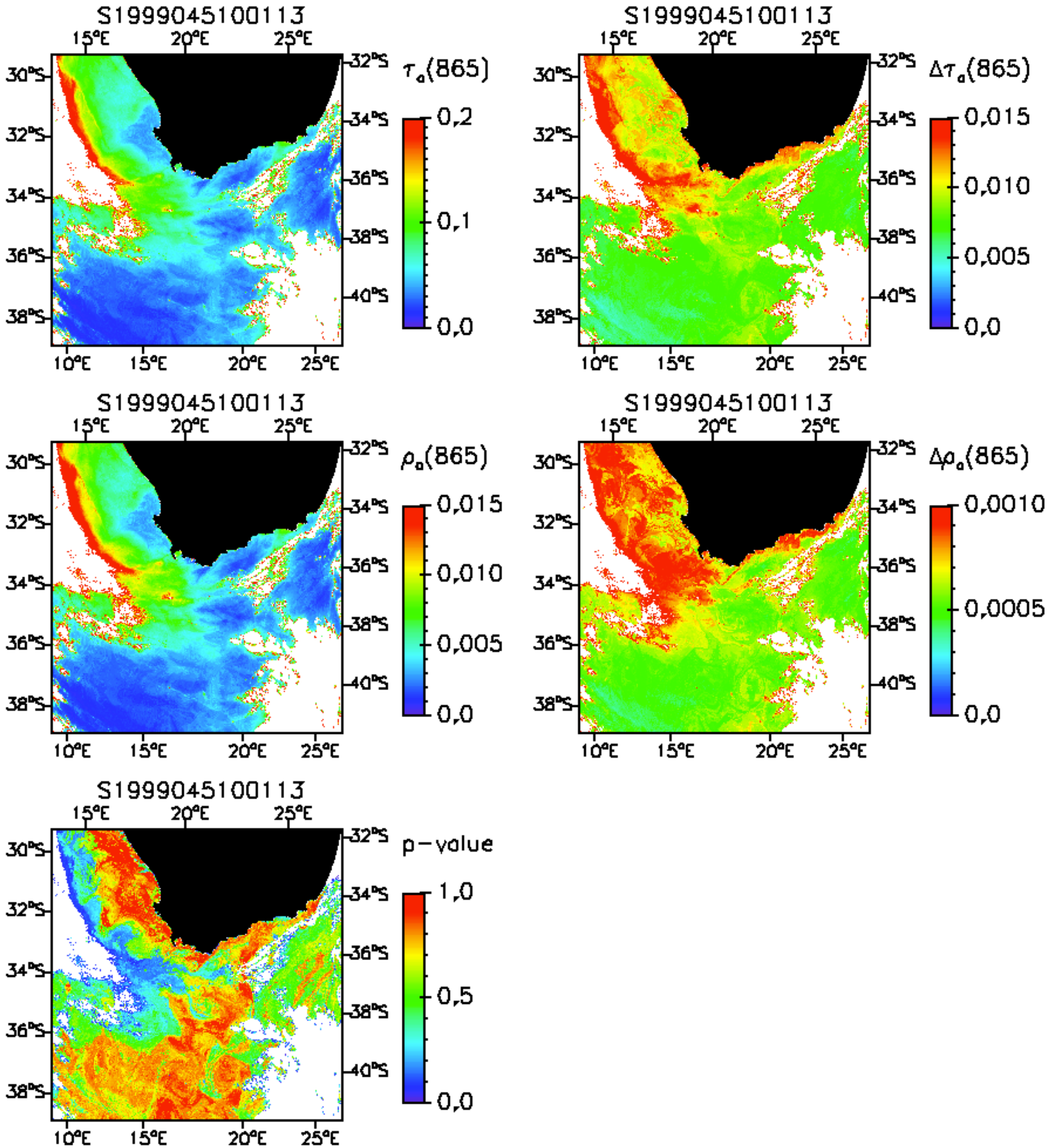

Estimated τ_a, ρ_a, and associated uncertainties, and p-value, Bayesian methodology.

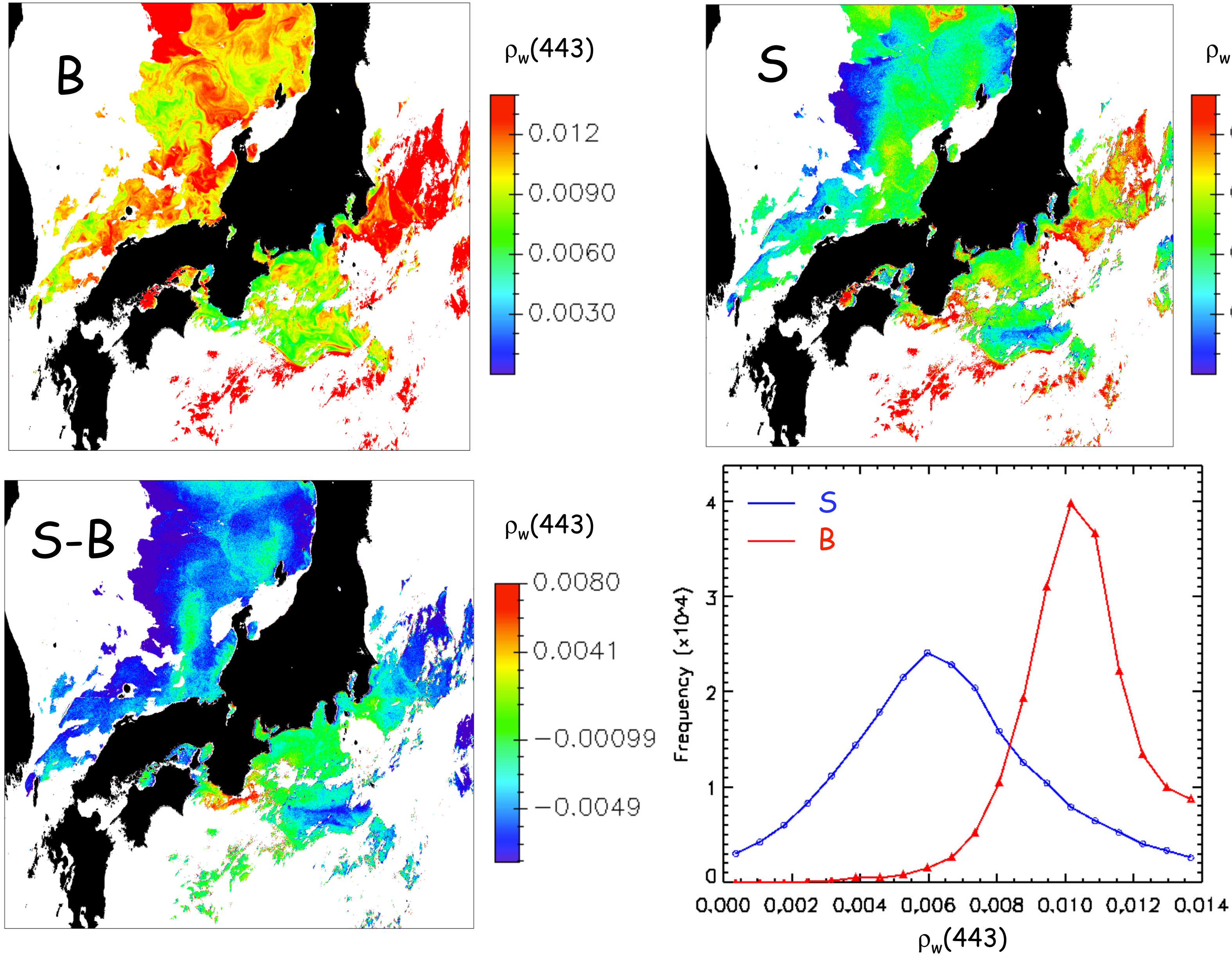

Estimated $\rho_w(443)$, Sea of Japan, 7 Aril 2001, in the presence of absorbing aerosols.

Comparison with in situ measurements

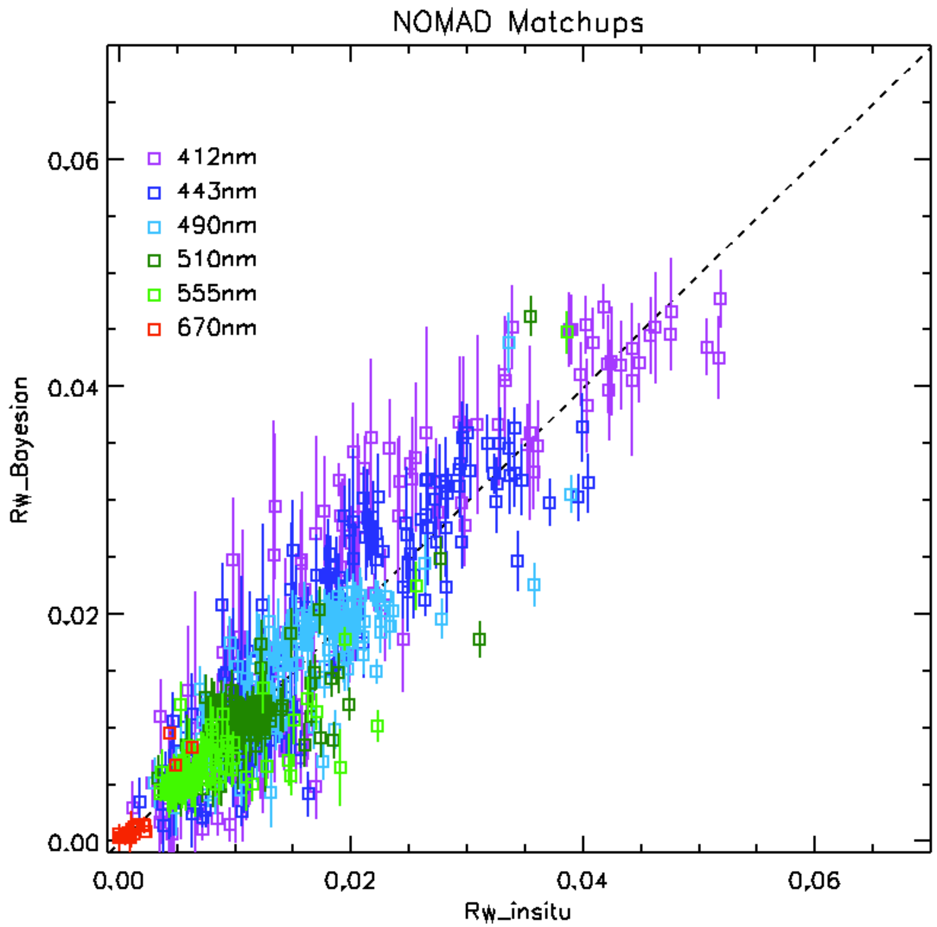

λ(nm)	R^2	Bias	RMSD	N
412	0.838	0.0016	0.0059	132
443	0.806	0.0009	0.0045	144
490	0.671	-0.0002	0.0034	144
510	0.587	-0.0005	0.0030	113
555	0.722	-0.0007	0.0026	129
670	0.820	<0.0001	0.0012	28
All	0.852	0.0002	0.0040	690

Comparison between marine reflectance estimated from SeaWiFS data using the Bayesian technique and measured in situ (NOMAD match-ups).

Future Work

-Further evaluation against in situ measurements.

-Application to imagery contaminated by Sun glint, thin clouds, and sea ice.

-Inclusion of information in the UV and shortwave infrared.

-Extension to very turbid waters.

-Regionalization (e.g., by including explicit knowledge of the space and time variability of atmospheric variables).

Estimation of the fraction of PAR absorbed by phytoplankton

-Primary production, *PP*, or the quantity or organic matter synthesized by phytoplankton per unit of surface and time, depends on the photo-synthetically available radiation absorbed by live phytoplankton, APAR. It can be modeled as:

$$PP = e \; APAR \; PAR$$

-Consider vertically homogeneous ocean, Case 1 waters. APAR can be expressed as:

$$APAR = \int [1 - R_w(\lambda)] \, E(\lambda) a_p(\lambda) / (a_t(\lambda) \, d\lambda \; / \int E(\lambda) \, dl$$

$$APAR \approx \int [a_p/(a_d + a_p)] \, [1 - (R_w / R_{w0}) \, b_{b0}/(b_{b0} + b_{bp})] \, E \, d\lambda \; / \int E \, d\lambda$$

Suggests that APAR can be estimated from a linear combination of R_w's in the PAR spectral range

Simulations

-Morel/Maritorena R_w model, variable phytoplankton type, chlorophyll concentration from 0.03 to 3 mg/m^3.

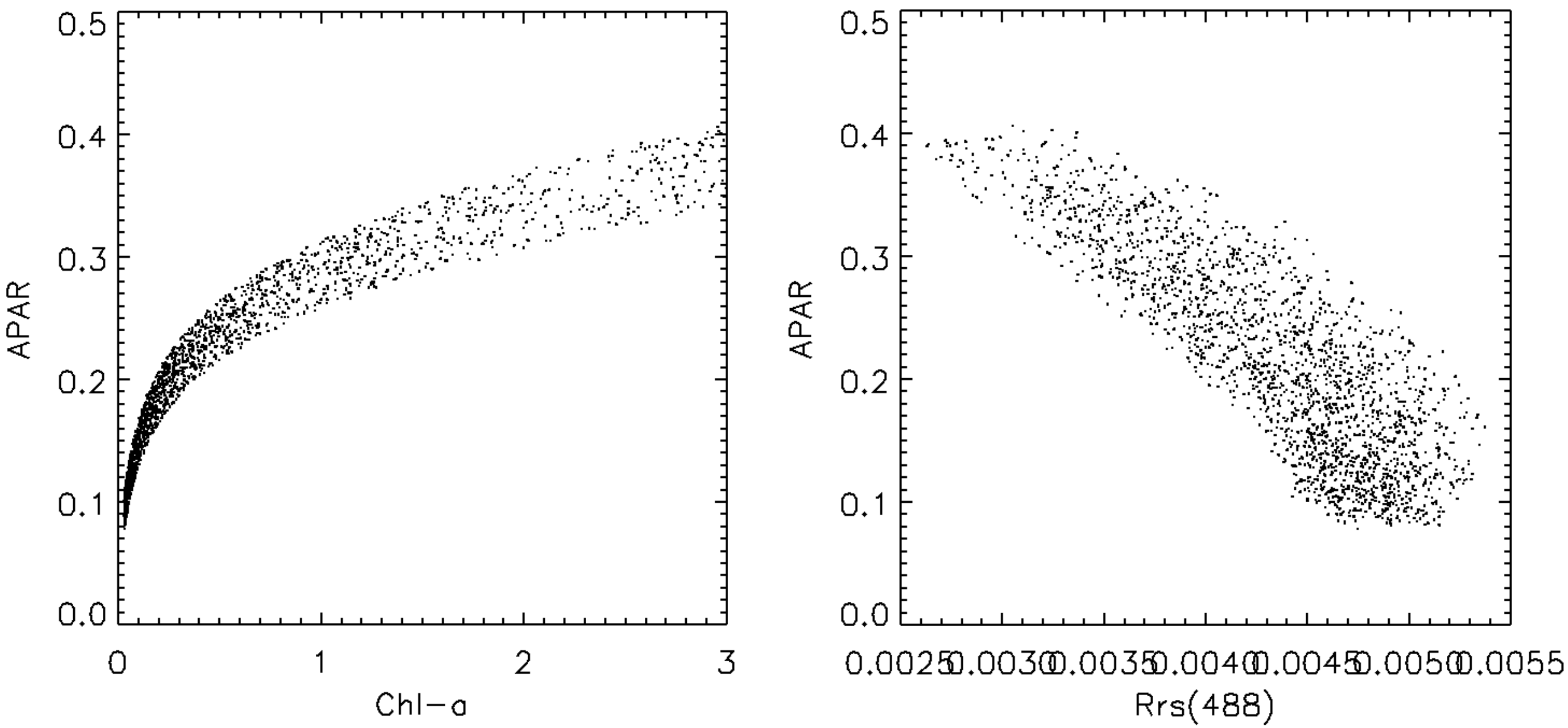

Simulated APAR as a function of Chlorophyll concentration (left) and remote sensing reflectance at 488 nm (right).

Multi-linear algorithm

$$APAR = a_0 + \Sigma_i a_i R_w(\lambda_i)/R_{w0}(\lambda_i), i = 1,\ldots,N$$

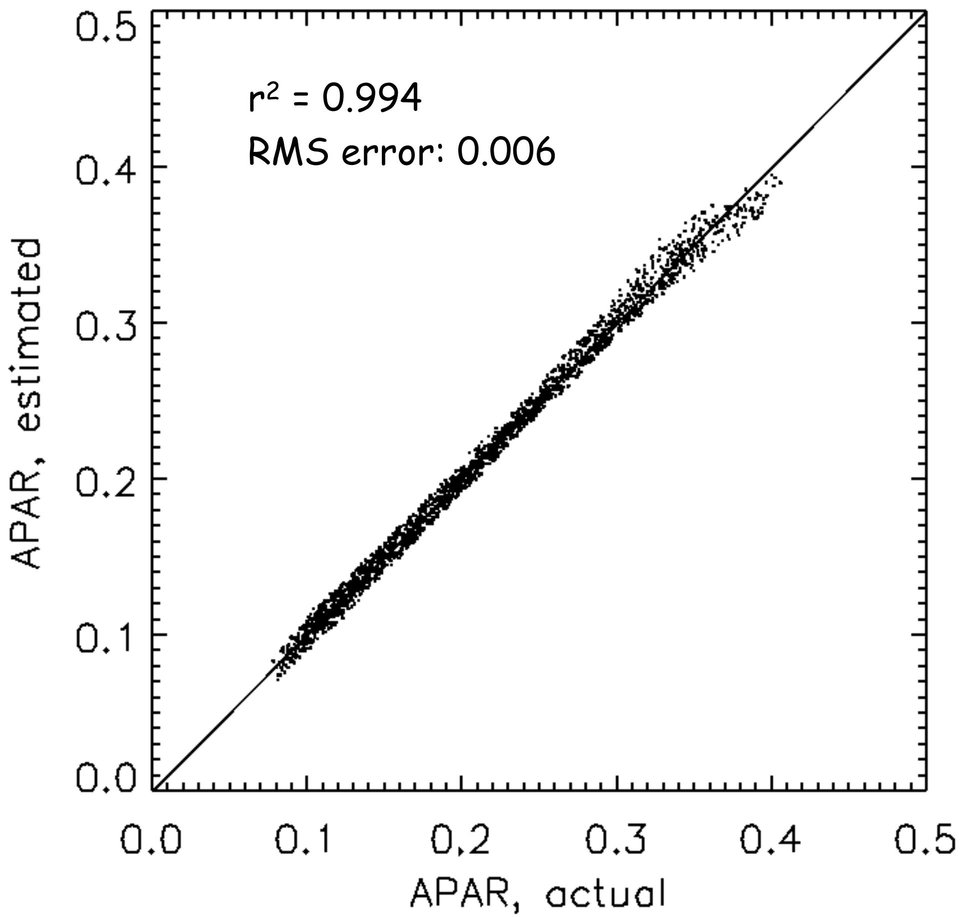

$$\begin{aligned} APAR = 0.327 & \\ &+ 0.456\, R_w/R_{w0}(412) \\ &- 0.862\, R_w/R_{w0}(443) \\ &+ 0.127\, R_w/R_{w0}(488) \\ &- 0.158\, R_w/R_{w0}(531) \\ &+ 0.150\, R_w/R_{w0}(555) \end{aligned}$$

Theoretical performance of algorithm to estimate APAR from marine reflectance at 412, 443, 488, 531, and 555 nm.

Application to MODIS Imagery

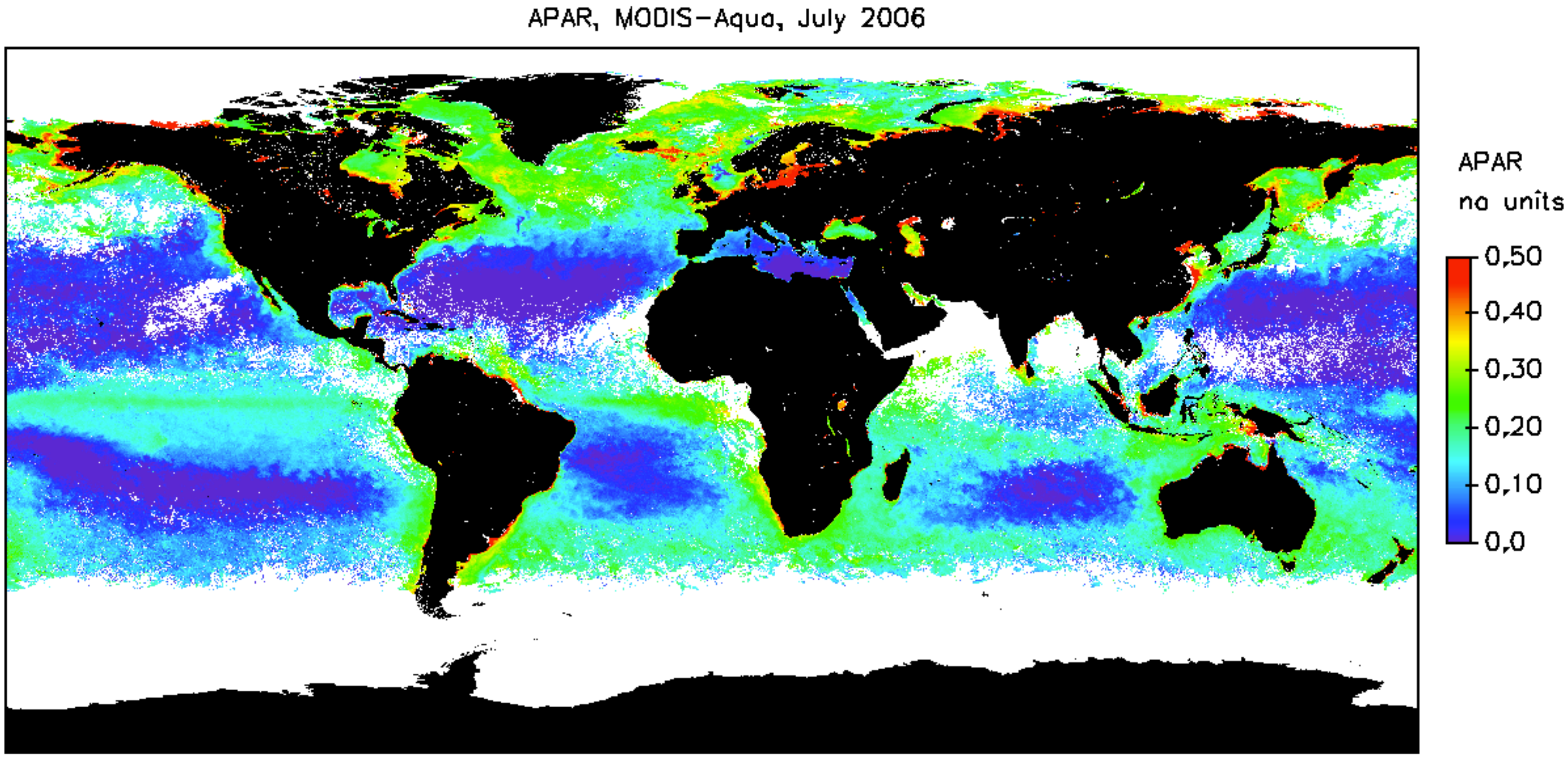

Monthly APAR estimated from a linear combination of marine reflectance at 412, 443, 488, 531, and 555 nm.

Future work

-Sensitivity to R_w noise.

-Optimization of band combination.

-Extension to vertically heterogeneous ocean.

-Comparison with other methods (e.g., using satellite Chl-a and IOP estimates).

-Evaluation against in-situ measurements.

Bio-optical Cruises

-*Accomplished*:

•VALHYBIO, IRD, 03/22/08-04/09/08, New Caledonia (Southwest lagoon). (Data processed.)

•MV1102, SIO, 02/20/11-13/03/11, Cape Town (South Africa) to Valparaiso (Chile). (Data processed.)

•CALIOPE1, IRD, 05/10/11-12/10/11, New Caledonia (East Coast), 21°S, 166°E. (Data processed.)

•VITEL1, IRD/LOG, 11/07/11-11/18/11, North Vietnam, 20°30'N, 107°E. (Data Processed.)

•POINTSUR, UABC/SIO, 04/19/13-04/26/13, Gulf of California, 23°S, 109°W. (Optical data Processed.)

•SPOT 1-2 and 4-5, IRD, 10/08/12-10/12/12, 02/08/13-02/13/13, 10/09/13-10/12/13, 12/05/13-12/10/13, Southwest Pacific, 20°S, 168°E. (SPOT-1 data processed.)

-Planned:

•SPOT 6-8, IRD, 03/02/14-03/06/14, 10/3/14-10/7/14, 12/3/14-12/7/14, Southwest Pacific, 20°S, 168°E.

•CALIOPE 2, IRD, 03/7-08/03 2013, 21°S, 166°E, New Caledonia (East Coast).

•COMéVA, IRD 10/14 (TBD), 16°S, 168°E, Vanuatu.

•OUTPACE, IRD, 02/15 (TBD), Nouméa (New Caledonia) to Papeete (Tahiti).

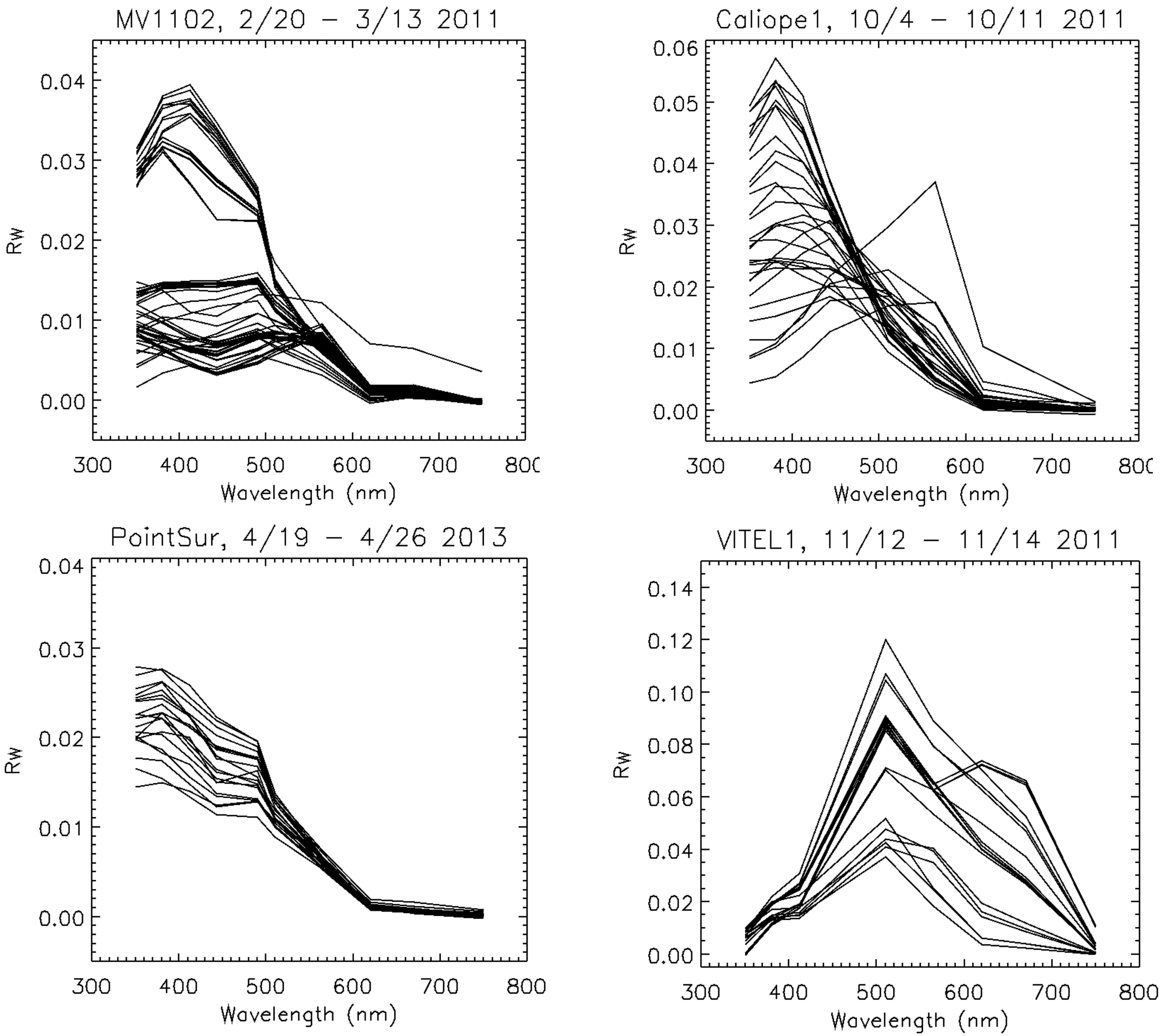

Examples of marine reflectance data sets collected by SIMBADA.

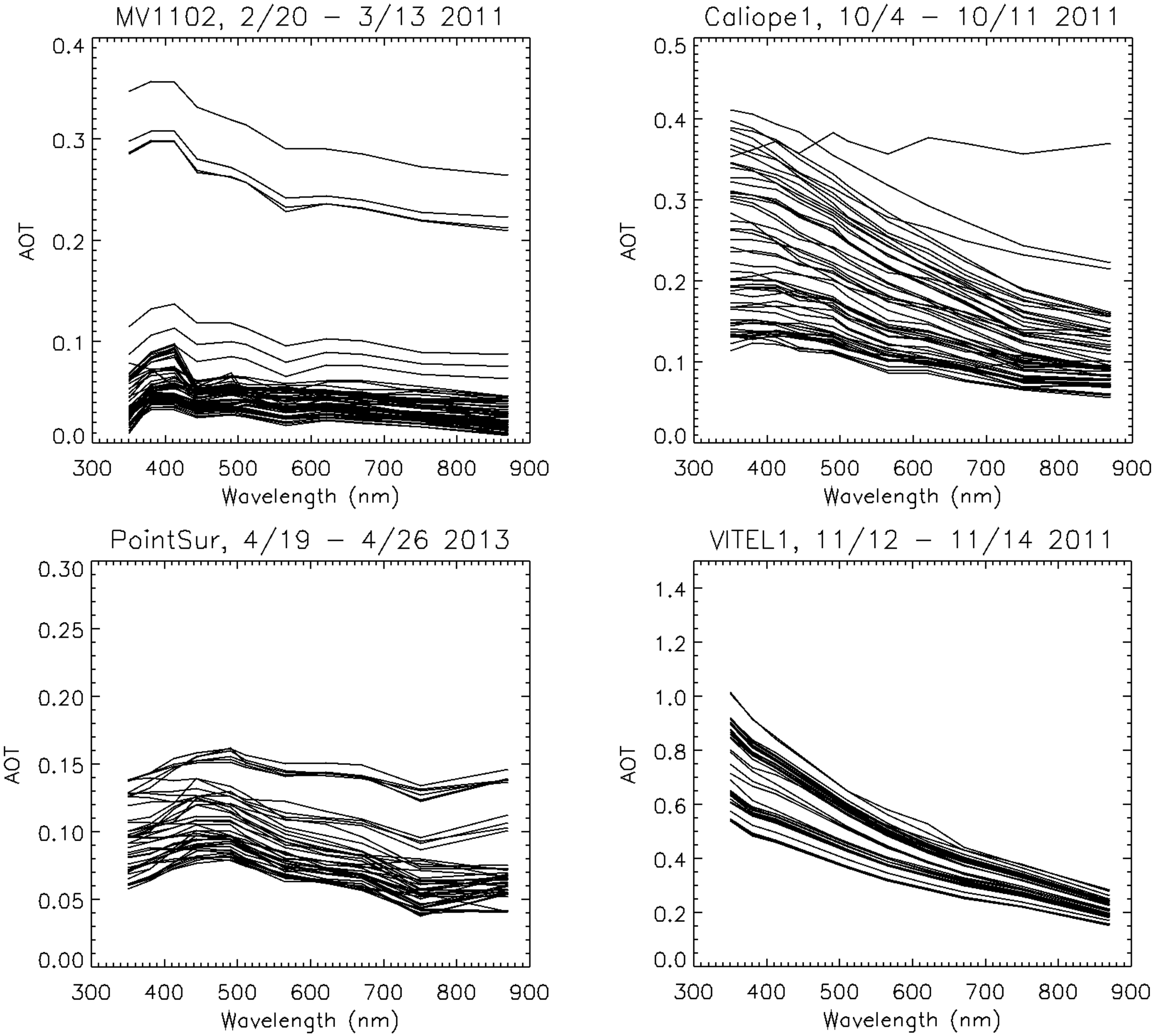

Examples of aerosol optical thickness data sets collected by SIMBADA.